ADVANCED HEALTHCARE MATERIALS
www.advhealthmat.de

Lipase-Sensitive Transfersomes Based on Photosensitizer/Polymerizable Lipid Conjugate for Selective Antimicrobial Photodynamic Therapy of Acne

*Hyung Park, Jonghwan Lee, Songhee Jeong, Byeong Nam Im, Min-Kyoung Kim, Su-Geun Yang, and Kun Na**

Acne vulgaris is a common skin problem affecting nearly 90% of adolescents and its development is associated with a colonization of *Propionibacterium acnes* (*P. acnes*). Although antibiotics have commonly been used to treat acne, antibiotic resistance of *P. acnes* is an emerging issue to be solved. In this study, a new way of photodynamic acne therapy is developed using *P. acnes* lipase-sensitive transfersome (DSPE-PEG-Pheo A (DPP) transfersome). For enhanced selectivity and skin penetration efficiency, DPP transfersomes are prepared from 1,2-distearoyl-*sn*-glycero-3-phosphoethanolamine-*N*-[amino(polyethylene glycol)-2000], pheophorbide A (Pheo A), cholesterol, and Tween-80. Incorporation of Tween-80 as an edge activator increases the deformability of DPP transfersomes, enhancing skin penetration efficiency to four times that of free Pheo A. The photoactivity of Pheo A quenched by DPP transfersomes is gradually recovered by selective cleavage of the ester linkage in DPP transfersomes by *P. acnes* lipases. In vitro *P. acnes*-specific photoactivity and subsequent selective antimicrobial effect exhibit a greater than 99% loss of *P. acnes* viability. In vivo antiacne therapeutic effect is confirmed by reduction of swelling volume and thickness of *P. acnes*-induced nude mice skin. These results demonstrate that DPP transfersome-mediated photodynamic therapy can be used as an alternative method to treat bacterial skin infections.

1. Introduction

Acne is a skin disorder experienced by 80%–90% of the population. Acne is caused by a variety of factors, such as acne-inducing bacteria, excess sebum production, and follicular epidermal hyperproliferation.[1–4] Free fatty acids formed through the hydrolysis of sebum triglycerides by *Propionibacterium acnes* (*P. acnes*) lipase promote the disruption of follicular epithelium and lead to inflammatory acne.[5–8] Antibiotics such as lincomycin, erythromycin, and tetracycline have been used to treat *P. acnes*. However, antibiotics have been reported to cause undesirable side effects such as vomiting, sore mouth, liver toxicity, erythema, diarrhea, gastrointestinal disorders, and skin redness.[9,10] Moreover, antibiotic resistance is continually occurring due to the overuse of antibiotics.[11–13] Antibiotic resistance has reached a critical level as major antibiotics used in clinics no longer work to treat patients.[14,15]

Recently, photodynamic therapy (PDT) has been developed as an alternative antimicrobial strategy for acne treatment.[16–18] PDT involves the combination of a photosensitizer (PS) and a light source. Absorption of adequate light excites the PS, and the excited PS reacts with molecular oxygen to generate singlet oxygen and reactive free radicals, which damage and destroy microorganisms.[19–21] The potential advantages of PDT induce a lower risk of developing side effects and antibiotic resistance. However, the PS treatments have a low degree of selectivity for killing microbial compared with host mammalian cells. Moreover, due to the low penetration efficiency of PSs into the skin, PSs cannot effectively treat deep skin bacteria.[22,23] Although PSs show antimicrobial effect, the insolubility of PSs in aqueous media restricts its clinical applications.[24,25]

To overcome these problems, we developed a self-quenching PS-conjugated lipid-based transfersomal carrier to achieve increased solubility and skin penetration efficiency of PSs. The carrier (DPP transfersome) was composed of 1,2-distearoyl-*sn*-glycero-3-phosphoethanolamine-*N*-[amino(polyethylene glycol)-2000] (DSPE-PEG(2000)-NH_2), pheophorbide A (Pheo A), cholesterol, and Tween-80. The advantages of the DPP transfersome include improved solubility of PS, enhanced skin penetration of PS, and control of the *P. acnes* lipase-responsive photoactivity. Transfersomes are deformable carriers that are able to pass through intercellular spaces in the stratum corneum smaller than their own size.[26,27] Transfersomes that contain edge

Dr. H. Park, Dr. J. Lee, S. Jeong, B. N. Im, Prof. K. Na
Center for Photomedicine
Department of Biotechnology
The Catholic University of Korea
43 Jibong-ro, Wonmi-gu
Bucheon-si, Gyeonggi-do 420-743, South Korea
E-mail: kna6997@catholic.ac.kr
Dr. M.-K. Kim, Prof. S.-G. Yang
Department of New Drug Development
School of Medicine
Inha University
2F A-dong, Jeongseok Bldg., Sinheung-dong 3-ga
Jung-gu, Incheon 400-712, Republic of Korea

DOI: 10.1002/adhm.201600815

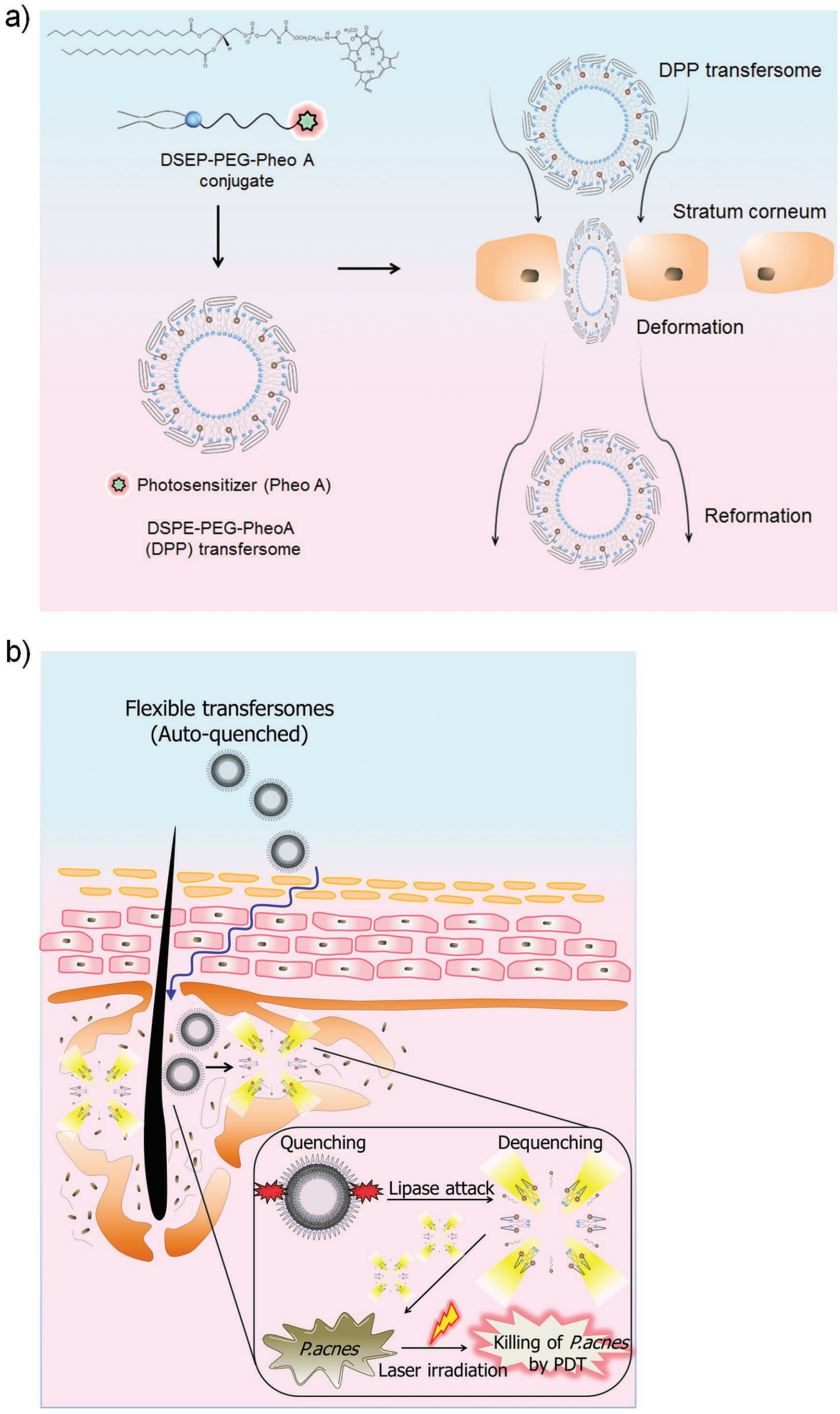

Scheme 1. Schematic illustrations of a) skin penetration and b) lipase sensitivity and recovery of photoactivity of the DPP transfersomes.

activators within lipid bilayers show increased deformability and flexibility. When applied to the skin, the transfersomes are able to deform and squeeze between the intercellular spaces of the stratum corneum.[26,28] Consequently, transfersomes improve both the interactions with skin and the transdermal efficiency of drug permeation (**Scheme 1**a). The DPP transfersome was also developed to show controllable photo activity of the PS in a lipase-abundant environment. During skin penetration, the photoactivity of the PS was completely quenched by the hydrophobically aggregated DPP transfersomes. Selective recovery of the quenched photoactivity of Pheo A is achieved by *P. acnes* lipase in the dermis layer of *P. acnes*-induced skin. *P. acnes* lipases specifically cleave the ester linkage of phospholipid molecules in the DPP transfersomes and induce structural disruption of the DPP transfersomes. These processes eventually lead to photoactivity dequenching. Finally, additional laser irradiation specifically eliminates *P. acnes* (Scheme 1b).

2. Result and Discussion

2.1. Preparation and Characterization of the DPP Transfersomes

To prepare the photosensitizer-conjugated lipid, Pheo A was conjugated with DSPE-PEG(2000)-NH_2 through a conventional carbodiimide reaction in chloroform (**Scheme 2**). The formation of DSPE-PEG-Pheo A (DPP) conjugates was verified by ^{1}H NMR (500 MHz, dimethyl sulfoxide (DMSO)-d_6). The peaks of DSPE-PEG-2000 were observed at δ, ppm 4.02 (CH_2OCONH, 2H), 3.50–2.25 (−NH, 1H, $-NH_2$, 2H, $-NH_3$, 3H), between 6.7 and 2.1–1.9 (−CH, 3H, $-CH_2$, 1H), 0.84 ($-CH_3$, 6H), and 1.29 ($-CH_2CH_2CO$, 4H) (Figure S1, Supporting Information). After conjugation of DSPE-PEG(2000)-NH_2 with Pheo A, the amine peak (δ, ppm = 2.25) of the DPP conjugate disappeared. These results indicate that the DPP conjugates were successfully synthesized.

The DPP transfersomes were prepared from DPP conjugate, cholesterol, and Tween-80 via the thin-film hydration method. The size and morphology of the DPP transfersomes were examined by field emissions-canning electron microscope (FE-SEM) and dynamic light scattering (DLS). The DPP transfersomes were monodispersed with uniform morphology (**Figure 1**a). The average diameter of the DPP transfersomes was Z174.9 ± 30.5 nm (Figure 1b). The stability of the DPP transfersomes was evaluated during 14 d of incubation in phosphate buffered saline (PBS buffer, pH 7.4) (Figure S2, Supporting Information). During the incubation, the DPP transfersomes were fully dispersed and stable in aqueous solutions without forming any solid precipitates. The concentration of Pheo A in the DPP conjugates was analyzed by UV–vis spectrophotometry using a standard curve of free Pheo A at 406 nm and determined to be 0.16 mg Pheo A/1 mg of DPP conjugate (Figure S3, Supporting

Adv. Healthcare Mater. **2016**,
DOI: 10.1002/adhm.201600815

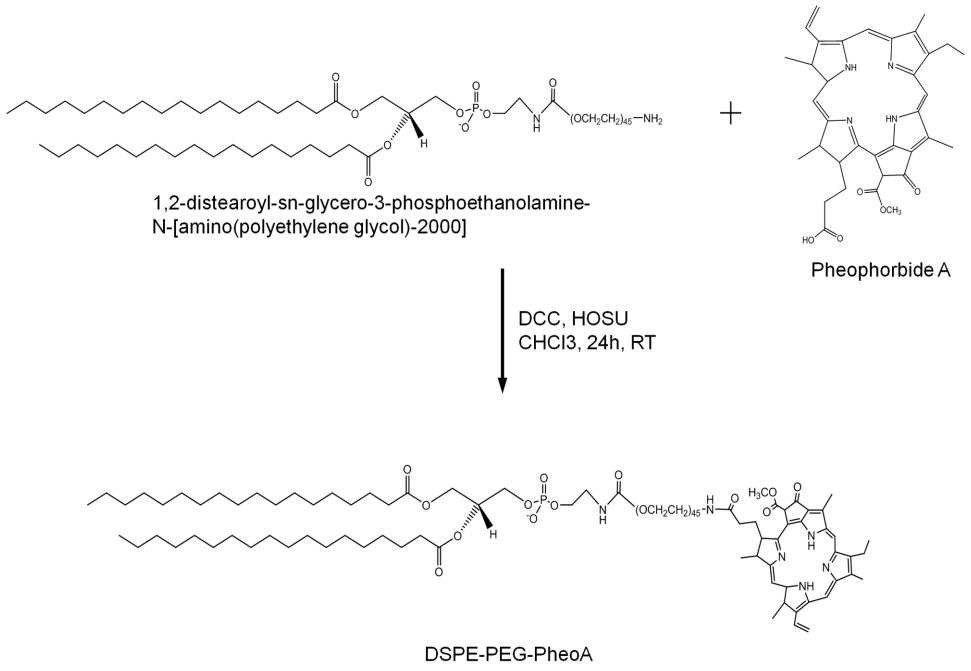

Scheme 2. Schematic of the procedure for synthesizing DPP conjugates.

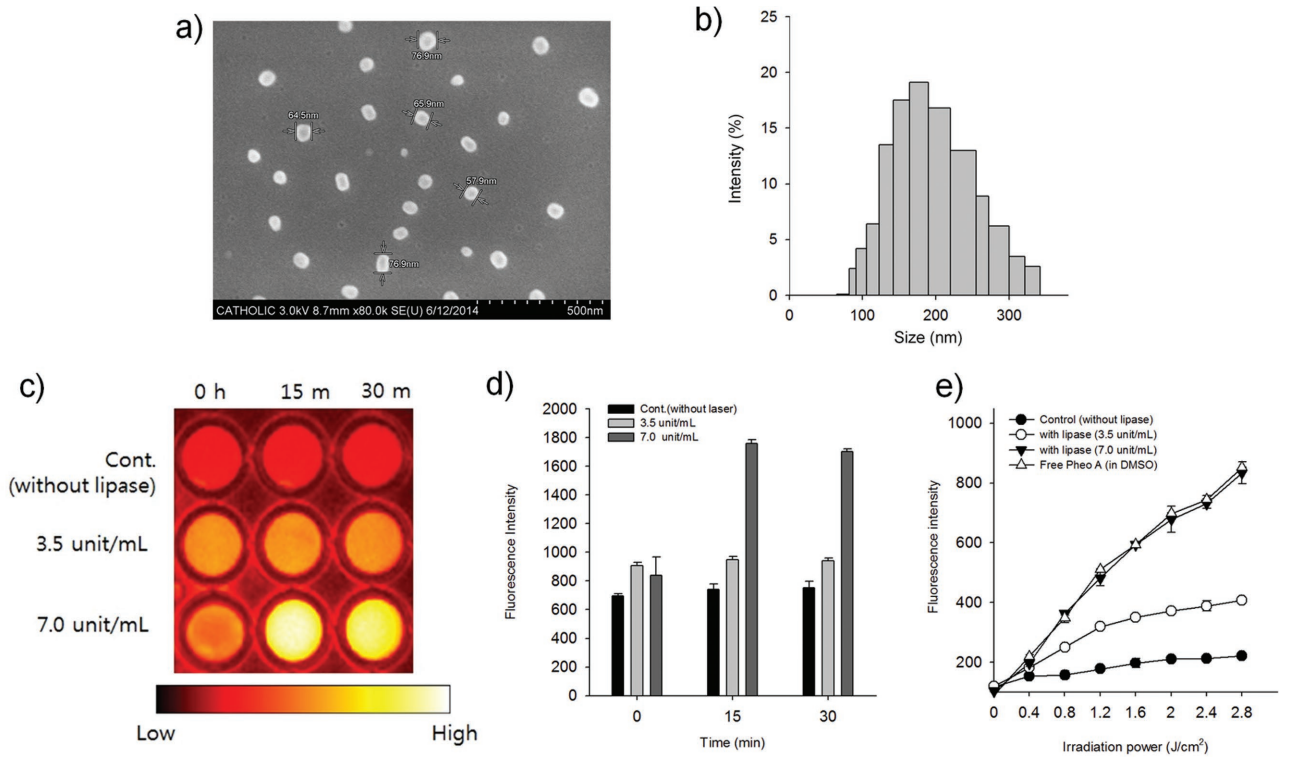

Figure 1. Characterization of the DPP transfersomes. a) FE-SEM image (scale bar = 500 nm). b) DLS analysis. The average diameter of the DPP transfersomes was determined to be 174.9 ± 30.5 nm. c) Recovery of photoactivity of Pheo A. The DPP transfersomes were treated with different concentrations of lipase. The recovery of quenched fluorescence intensity of Pheo A was lipase concentration-dependent ($n = 3$). d) Quantitative analysis of Pheo A fluorescence recovery. e) SOG efficiency of the DPP transfersomes in the presence or absence of lipase with different laser irradiation conditions. (light: 20 mW and 635 nm; SOSG Ex/Em: 504 nm/525 nm, $n = 3$).

Information). In addition, the DPP transfersomes did not affect the viability of NIH/3T3 cells. Compared with free-Pheo A, treatment with high concentration of the DPP transfersomes (up to 100 μg mL^{-1} of Pheo A) showed no significant decrease in cell viability (Figure S4, Supporting Information).

2.2. Lipase-Mediated Activation of the DPP Transfersome Photoactivity

To evaluate the lipase-sensitive self-quenching and dequenching of Pheo A in the DPP transfersome, the fluorescence intensity of Pheo A was measured with and without treating the DPP transfersomes with *Candida rugosa* lipase. In the absence of lipase, the fluorescence signal of Pheo A in the DPP transfersomes was low because the photoactivity of Pheo A was self-quenched by the fluorescence resonance energy transfer (FRET) effect induced by the highly aggregated structure of the DPP transfersomes (Figure 1c,d). As the lipase concentration increased, the fluorescence signals of Pheo A in the DPP transfersomes also increased. At a lipase concentration of 7.0 unit mL^{-1}, the fluorescence signal increased approximately twofold, while the effect of 3.5 unit mL^{-1} of lipase was not as significant. These results demonstrate that the structure of the synthesized DPP transfersomes was highly sensitive to lipase concentration. Furthermore, they revealed that at least 7.0 unit mL^{-1} of lipase and 15 min of treatment time was required to induce disintegration of the DPP transfersome and subsequent recovery of the photoactivity of Pheo A.

These results are important due to one of the drawbacks of PS-mediated PDT for dermal disease treatment is the uncontrollable photoactivity of PS, which may damage normal tissues. Therefore, developing a carrier system for PDT that has controlled on/off photoactivity is valuable for targeted PDT applications. The photoactivity of a PS should be completely quenched until it reaches the target site.[29] After reaching the target site, the self-quenched photoactivity of the PS should be recovered selectively by environmental factors such as enzymatic activity, pH change, and expression of specific nucleic acids or proteins.

2.3. Evaluation of Singlet Oxygen Generation (SOG) Efficiency

SOG efficiency is one of the critical factors of the DPP transfersomes because the generation of reactive oxygen species-mediated oxidative stress results in bacterial cell death. To investigate the SOG efficiency of the DPP transfersomes in the presence or absence of lipase in the aqueous phase, singlet oxygen sensor green (SOSG, S-36002; Invitrogen/Molecular Probes) was used as an indicator. SOSG was selected because it reacts with singlet oxygen and emits green fluorescence signal.[30]

When treated without or with low (3.5 unit mL^{-1}) lipase activity, the fluorescence intensities of the SOSG in the DPP transfersomes were very low under various laser irradiation conditions due to the FRET effect (Figure 1e). Whereas, a significant increase in SOSG fluorescence intensity was observed in the DPP transfersomes treated with high concentrations (7.0 unit mL^{-1}) of lipase; the fluorescence was almost the same as that of free Pheo A in organic solvent (DMSO). These results indicate that a high concentration of lipase effectively induced DPP transfersomes disruption and subsequent dequenching of Pheo A. The increase in SOSG fluorescence intensity is attributed to the singlet oxygen species generated via the liberated Pheo A. These results further demonstrate that the conjugated Pheo A in the DPP transfersomes successfully maintained its singlet oxygen generating photoactivity.

2.4. Skin Penetration Efficiency of the DPP Transfersomes

For effective *P. acnes* therapy, PSs need to penetrate into the dermis, where *P. acnes* is primarily located. To investigate skin penetration efficiency, free Pheo A, Pheo A-loaded α-dipalmitoylphosphatidylcholine (DPPC) liposomes, and DPP transfersomes (1.0 μg mL^{-1} of Pheo A concentration, respectively) were treated on the mouse back skins. After 24 h of treatment, cross sections of each skin layer from the back skin of hairless mice and *P. acnes*-induced skin from the Franz cell diffusion system were analyzed using confocal microscopy.

Fluorescence of free Pheo A was only detected in the stratum corneum and not in the dermis of both normal and *P. acnes*-induced skins due to the low solubility and high molecular weight of free Pheo A (**Figure 2**). Pheo A is hydrophobic and has very low solubility in the aqueous phase. The molecular weight of Pheo A, 592.68 Da, also causes poor skin penetration efficiency as the molecular weight of a compound should be lower than 500 Da for effective skin absorption.[31] Pheo A-loaded liposomes showed higher skin penetration efficiency than free Pheo A because they are composed of DPPC, which has a composition similar to that of the cell membrane. However, Pheo A-loaded liposomes were detected in the dermis, stratum corneum, and epidermis. The detection of Pheo A-loaded liposomes in the stratus corneum and epidermis is most likely due to a release of Pheo A during skin penetration. This biodistribution of the PS may become a limiting factor for liposome-mediated PS delivery in clinical use. Randomly distributed PS may cause long-lasting skin toxicity or off-target toxicity.[32–35]

Interestingly, fluorescence of Pheo A in the DPP transfersomes was only detected in the dermis of *P. acnes*-induced skin. Specific delivery of PS to the dermis of *P. acnes*-induced skin was achieved by the increased deformability and hydrophilicity of the DPP transfersomes. Tween-80 was used as an edge activator in the DPP transfersomes. Edge activators are incorporated into the lipid bilayers of transfersomes to enhance structural flexibility and deformability, allowing the transfersomes to squeeze between the intercellular spaces of the stratum corneum.[36,37] The enhanced hydrophilicity provided by PEG let the transfersomes experience less osmotic stress and transfer the PS to the dermis of *P. acnes*-induced skin.[38,39]

The dermis region-specific distribution of Pheo A fluorescence further demonstrated that the photoactivity of Pheo A was recovered through *P. acnes* lipase-mediated disruption of the DPP transfersomes in the *P. acnes* infected environment. Therefore, the DPP transfersomes are effective for the transdermal delivery of PS to the target dermis and for the environmental condition-responsive restoration of photoactivity in the target region.

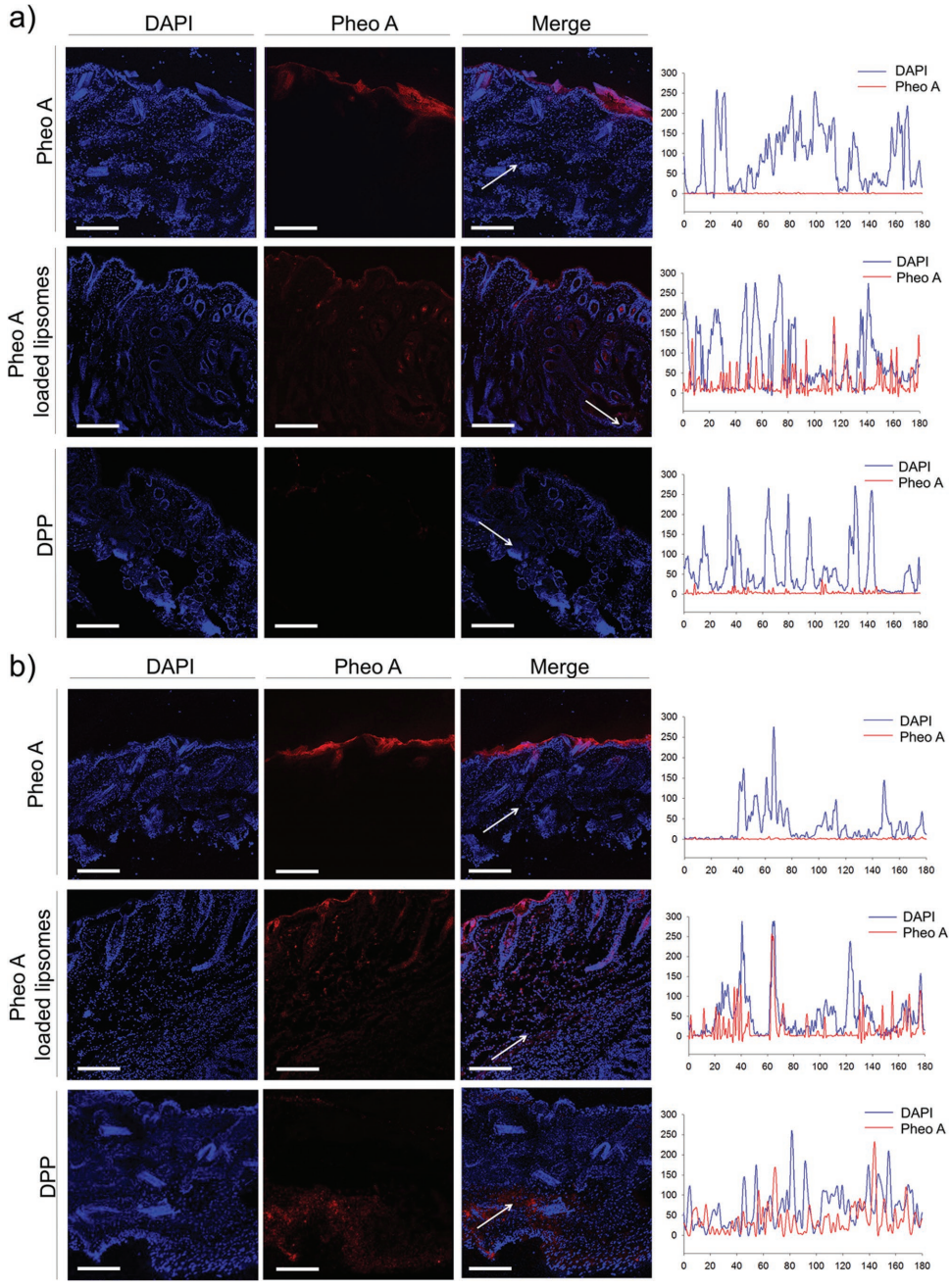

Figure 2. Confocal microscopic analysis to compare skin penetration efficiency of free Pheo A, DPPC liposomes, and the DPP transfersomes. The line scan data are shown by the white arrows in the images. Cross-sections of a) normal skin and b) *P. acnes*-induced skin were incubated on a Franz diffusion cell and analyzed ($n = 3$). The blue signal indicates 4′,6-diamidino-2-phenylinodle (DAPI) (nucleus; excitation/emission: 358/461 nm) and the red signal indicates Pheo A (excitation/emission: 410 nm/675 nm). Scale bars indicate 200 µm.

2.5. In Vitro Diffusion Assay

The minimal inhibitory concentration (MIC) of free Pheo A and the DPP transfersomes were characterized by an agar diffusion assay. Nonlaser-irradiated free Pheo A and DPP transfersomes with different concentrations (0, 0.05, 0.1, 0.5, and 1.0 µg mL^{-1} of Pheo A) did not show any effect on *P. acnes* growth. (Figure S5, Supporting Information). Inhibition of *P. acnes* growth was dependent on both Pheo A concentration and irradiation intensity. Below 0.10 µg mL^{-1} of Pheo A in each sample, a slight increase in bacterial death was observed. At Pheo A concentrations above 0.5 µg mL^{-1} and irradiation intensities above 0.5 J cm^{-2}, significant inhibition of *P. acnes* growth was detected. Although the inhibitory effects between two different concentrations (0.5 and 1.0 µg mL^{-1}) of Pheo A and among three different laser intensities (1.0, 2.0, and 4.0 J cm^{-2}) were quite similar, we selected 1.0 µg mL^{-1} of Pheo A and 4 J cm^{-2} laser irradiation for further investigations.

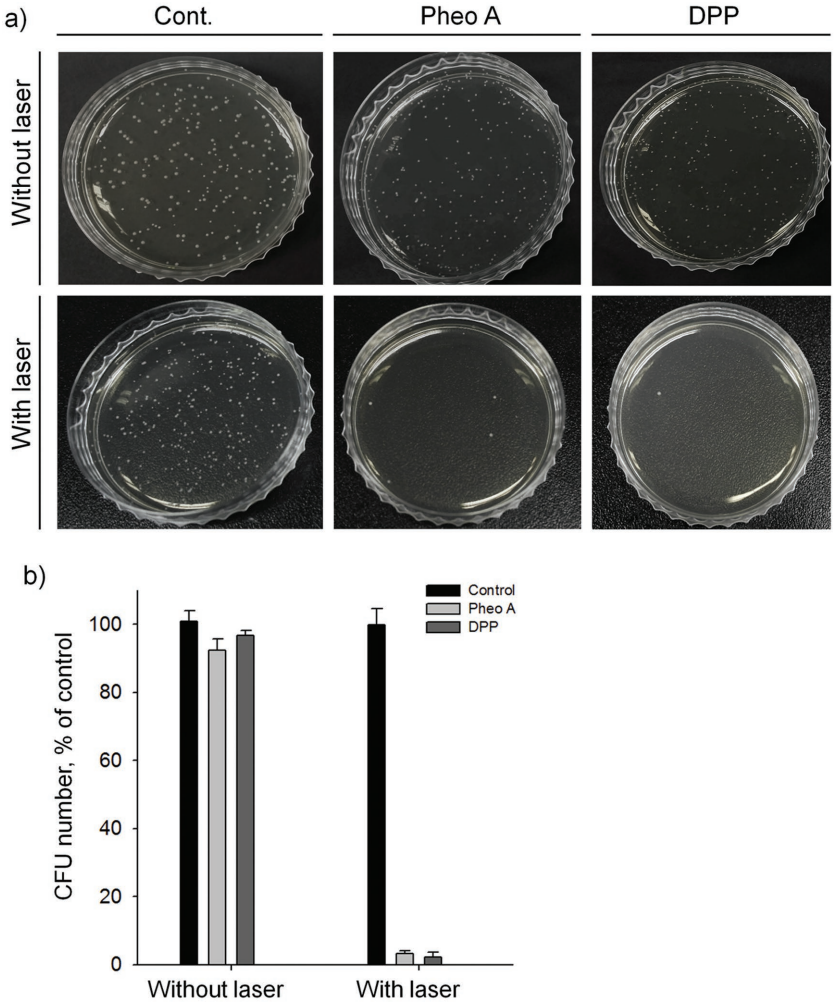

Figure 3. In vitro antibacterial effect of the DPP transfersomes. a) PBS buffer or free Pheo A (1 μg mL^{-1}) or the DPP transfersomes (1 μg mL^{-1} of Pheo A) were added to *P. acnes* suspensions. Followed by laser irradiation at 4 J cm^{-2} (20 mW cm^{-2} and 200 s), *P. acnes* was cultured on mRCM agar plates for 72 h. b) CFUs were quantitatively analyzed. Data are represented as means ± standard deviations of triplicate samples (**$p < 0.01$).

2.6. In Vitro Antibacterial Effect of the DPP Transfersomes by Colony Forming Units (CFU) Assay

Over 99% of *P. acnes* incubated with either free Pheo A (1.0 μg mL^{-1}) or DPP transfersomes (1.0 μg mL^{-1} of Pheo A) and then laser irradiated (4 J cm^{-2}) resulted in bacterial cell death (**Figure 3**). Without laser irradiation, there was no inhibitory effect on bacterial growth. The results indicate that treating with 1.0 μg mL^{-1} of free Pheo A and DPP transfersomes without irradiation had no toxic effect on *P. acnes* growth. The bactericidal effect of free Pheo A and DPP transfersomes was only observed after treatment with a laser. Laser irradiation triggered the Pheo A to generate singlet oxygen, which interacts with *P. acnes*, resulting in bacterial cell death.[40,41] These results also demonstrated that the incorporated Pheo A in the DPP transfersomes remained stable during DPP transfersome preparation, including DSPE-PEG and Pheo A synthesis and incubation with *P. acnes*.

2.7. In Vivo Antibacterial Effect of the DPP Transfersomes

To study the antibacterial effect of the DPP transfersomes on *P. acnes*-induced inflammation in vivo, *P. acnes* was intradermally injected into the back skin of nude mice. Significant skin swelling was observed in *P. acnes*-injected back skin ≈1 d after the injection. However, no swelling was detected in the PBS-injected back skin. Histological analysis showed that injection with *P. acnes* triggered a considerable increase in the number of infiltrated inflammatory cells (Figure S6, Supporting Information). With these results, we confirmed that the animal model of *P. acnes*-induced inflammation was fabricated successfully.

After skin swelling was observed, free Pheo A (1 μg mL^{-1}) or DPP transfersomes (1 μg mL^{-1} of Pheo A) were administered epicutaneously and irradiated. One day after laser irradiation, the swelling volume of the DPP transfersome-treated back skin was significantly reduced (**Figure 4**). However, without treatment of laser irradiation, the volume of the swollen skin continued to increase up to day 5. These results indicate the structure of the DPP transfersomes were specifically disrupted by *P. acnes* lipases and the subsequent bactericidal effect of Pheo A was selectively induced by laser irradiation. The in vivo antibacterial effect of the DPP transfersomes effectively reduced *P. acnes*-induced inflammation within 5 d. The effect of laser irradiation in the free Pheo A administered mice was not significant. The skin in laser-irradiated mice showed a reduction of ≈75%–85% of volume compared to nonirradiated mice. The different results for free Pheo A and the DPP transfersome under laser irradiated conditions was caused by the decreased skin penetration efficiency of free Pheo A (Figure 2).

Histological analysis showed a dramatic reduction of inflammatory cells in *P. acnes*-induced skin treated with DPP transfersomes and irradiated with a laser (**Figure 5**a). Skin treated with DPP transfersomes but not irradiated did not show a reduction of inflammatory cells. Similarly, the free Pheo A administered *P. acnes*-induced skins with or without treatment of laser irradiation showed no reduction in inflammatory cells. The inflammatory cell reduction efficiency of free Pheo A was not efficient for in vivo use.

Measuring the reduction of skin thickness further demonstrated the efficacy of DPP transfersomes. The skin thickness of the DPP transfersome administered region with laser irradiation was dramatically decreased compared to the thickness of untreated *P. acnes*-induced skin (Figure 5b,c). However, variation of skin thickness in the free Pheo A administered region was not so clear under both nonirradiated and irradiated

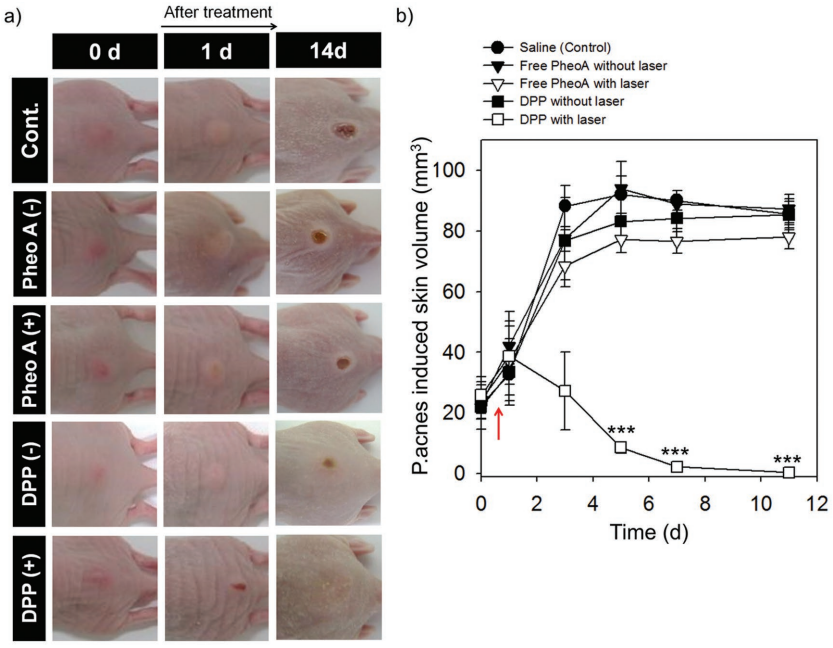

Figure 4. In vivo photodynamic therapy of acne using the DPP transfersomes. *P. acnes*-induced mice were treated with free Pheo A (1.0 μg mL^{-1}) or the DPP transfersome (1.0 μg mL^{-1} of Pheo A). For comparison, 144 J cm^{-2} (150 mW cm^{-2}, 16 min) of laser was irradiated (+) or nonirradiated (–). a) Images show the dramatic decrease in swelling volume of the DPP transfersome-treated back skin of *P. acnes*-induced mice after laser irradiation. b) Comparison of swelling volume size in the back skins of *P. acnes*-induced mice during the 11-day incubation period. The red arrow indicates the time of laser irradiation. ($n = 4$ mice per group). Data are represented as means ± standard deviations of samples (***$p < 0.005$).

conditions. Additionally, during the treatment period, side effects, such as erythema, scaling, and irritant dermatitis, were not detected due to photoactivity of the DPP transfersome restoration in target sites only.

The death of *P. acnes* was also evaluated by analyzing the number of *P. acnes* in the skin tissue at the end of treatment for all experimental groups. *P. acnes* did not grow in the DPP transfersome-mediated PDT group because the DPP transfersomes that reached the dermis were disrupted by lipase, resulting in singlet oxygen generation, and the killing of *P. acnes* (Figure S7, Supporting Information).

These results strongly suggest that epicutaneous application of the DPP transfersomes and subsequent laser irradiation can effectively and specifically suppress *P. acnes*-induced inflammatory cells and eliminate *P. acnes*, without causing side effects on surrounding skin cells. These findings are consistent with the previous report of an effective reduction of antiinflammatory cells by photosensitizer-mediated PDT.[42]

3. Conclusion

For use as a PDT-based acne treatment, *P. acnes* lipase-sensitive DPP transfersomes with an average diameter of 175 nm were prepared. For enhanced skin penetration and targeted delivery of Pheo A into the dermis of skin, PEG and Tween-80 were introduced to increase the surface hydrophilicity and structural deformability of the transfersomes, respectively. In the absence of lipase, the photoactivity of Pheo A was self-quenched due to the intramolecular interaction between closely packed Pheo A in the transfersome. Pheo A dequenching was selectively induced by *P. acnes* lipase-mediated disruption of the DPP transfersomes. Subsequent laser irradiation resulted in singlet oxygen generation and an antibacterial effect. The in vivo antibacterial effect of the DPP transfersomes was higher than that of free Pheo A. Ex vivo experiments further demonstrated that most of the *P. acnes* were eliminated by the DPP transfersome-mediated PDT. Therefore, the enzyme-sensitive and PS-quenching transfersomes may contribute to the development of new PDT-based acne treatments.

4. Experimental Section

Materials: DSPE-PEG(2000)-NH_2, DPPC, and cholesterol were purchased from Avanti polar lipids, Inc. Lipase from *Candida rugosa,* pheophorbide a (Pheo A), *N*-hydroxysuccinimide (NHS), 1,3-dicyclohexyl carbodiimide (DCC), Tween-80, and 3-(4,5-dimethylthiazol-2-yl)-2,5-diphenyltetrazolium bromide (MTT) were purchased from Sigma-Aldrich Corp (St. Louis, MO, USA). Dialysis membranes (MWCO: 1000) were obtained from Spectrum Laboratories Inc. (Rancho Dominguez, CA, USA). DMSO was purchased from Junsei Chemical (Tokyo, Japan). SOSG was purchased from Molecular Probes Inc. (Eugene, OR, USA). NIH/3T3 mouse fibroblast (ATCC CRL-1658) and *P. acnes* (ATCC 6919) were purchased from ATCC. Dulbecco's modified Eagle's medium (DMEM) was purchased from Thermo Scientific Hyclone (Utah, USA). Fetal bovine serum (FBS) and penicillin/streptomycin solution were purchased from Gibco(Grand Island, NY, USA).

Synthesis of DPP Conjugates: The DPP conjugates were synthesized via conventional carbodiimide reaction according to a previous report.[43] Briefly, DSPE-PEG(2000)-NH_2 (1 g) and Pheo A (100 mg) were dissolved separately in chloroform (20 mL) for 4 h. Next, NHS and DCC were added to the Pheo A solution as a catalyst and coupling reagent, respectively. After 4 h, the Pheo A solution was added dropwise into the DSPE-PEG(2000)-NH_2 solution and stirred for 24 h. After 24 h, the reaction solution was filtered for 3 d using a dialysis membrane with a 1K MWCO to remove insoluble byproducts (e.g., dicyclohexylurea). The solution was removed from the membrane, filtered, and lyophilized. The structure of the DPP conjugates was determined using a Bruker ^{1}H NMR (500 MHz, DMSO-d_6) spectrometer (Bruker, Germany).

Preparation and Characterization of the DPP Transfersome and Pheo A-Loaded DPPC Liposome: The DPP transfersomes were prepared using a thin-film hydration method.[44] The DPP conjugates, cholesterol (85%:15%, w/w), and Tween-80 (95%:5%, w/w) were dissolved in chloroform (5.0 mL) and transferred to a round bottom flask An evaporator was used at 40 °C to make a thin film on the walls of the flask. Next, 10% v/v ethanol in PBS (pH 6.5) was added to hydrate the lipid film and then film was stored overnight under high vacuum to remove any traces of solvent. The dried lipid film was rehydrated with 3 mL of deionized water. The lipid suspension was vortexed for 5 min and then sonicated for 30 min using a sonicator (VCX 750, Sonics&Materials, USA). The resulting vesicle suspension was sterilized by filtration through a 0.2 μm microporous filter (Poretics, CA, USA). The size and morphology of the DPP transfersomes were estimated using DLS (Zetasizer Nano ZS, Malvern Instruments Ltd., UK) and field emission-scanning electron microscopy (S-4700, Hitachi, Japan). To evaluate a colloidal stability of the DPP transfersomes, 1 mg mL^{-1} of the DPP transfersomes was incubated in PBS buffer (pH 7.4) for 14 d.

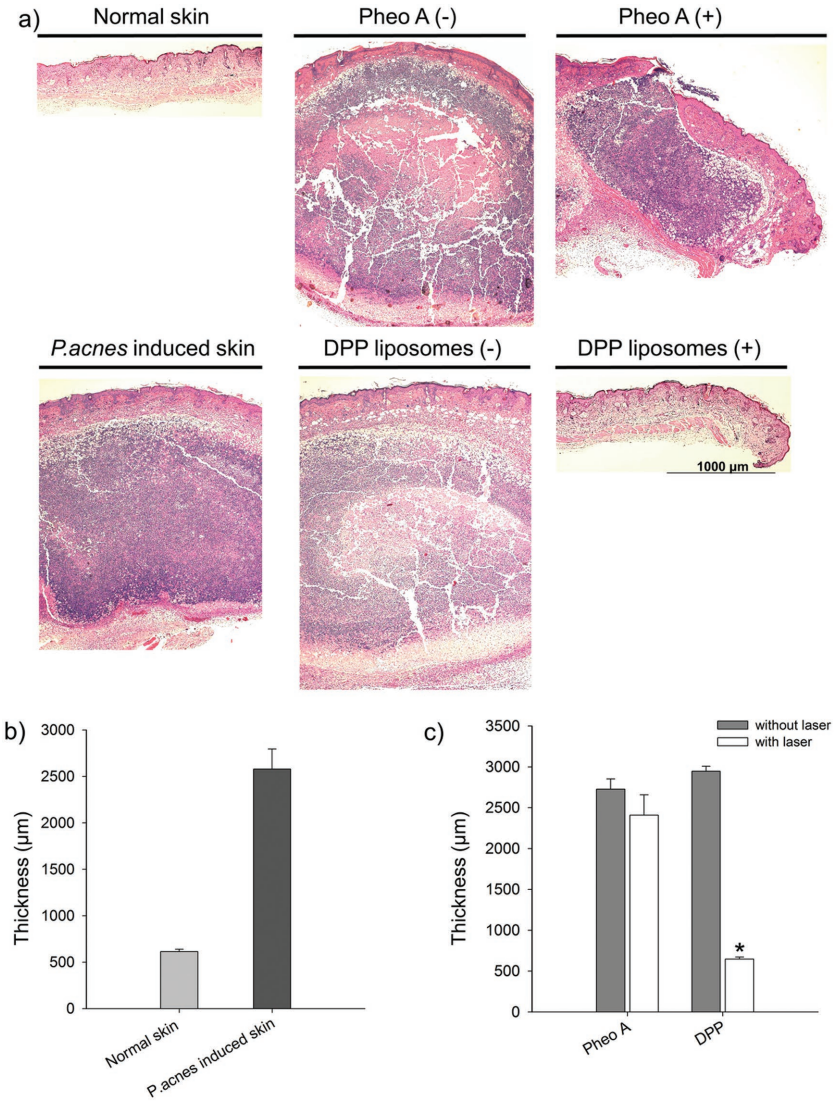

Figure 5. Reduction of the number of inflammatory cells and skin thickness. a) Histological analysis of skin tissues obtained from normal mice and *P. acnes*-induced mice. *P. acnes*-induced mice were treated with free Pheo A or the DPP transfersomes and laser was either irradiated (+) or nonirradiated (–). b) Quantitative analysis of thickness of normal skin and *P. acnes*-induced skin. c) Skin thickness of *P. acnes*-induced mice was further analyzed after treatment of free Pheo A or the DPP transfersomes under laser irradiated or nonirradiated conditions. ($n = 4$ mice per group, scale bar: 1000 μm). Data are represented as means ± standard deviations of samples ($^*p < 0.05$).

To evaluate the lipase-sensitive DPP transfersome photoactivity, the DPP transfersomes (Pheo A conc.; 1 μg mL^{-1}) were mixed with *Candida. rugosa* lipase (0–7 units mL^{-1}; Sigma-Aldrich Corp. St. Louis, MO, USA) at a 1:1 ratio and activated at 37 °C for 0–30 min. Fluorescence images of Pheo A were captured using a 12-bit charge coupled device camera (Image Station 4000 MM; Kodak, New Haven, CT, USA) with a special C-mount lens and a long-wave emission filter (600–700 nm; Omega Optical, Brattleboro, VT, USA).

Pheo A-loaded DPPC liposomes were synthesized using a thin-film hydration method. DPPC (10 mg), cholesterol (1.5 mg), and Pheo A (1 mg) were dissolved in chloroform (5 mL), and the mixture was transferred to round-bottom flask. An evaporator was used at 40 °C to make a thin film on the walls of the flask. Next, 1×10^{-3} M ammonium sulfate solution (10 mL) was used to hydrate the thin film. Finally, Pheo A-loaded liposomes were prepared by sonication.

Cell Culture and Cytotoxicity Test: NIH/3T3 cells were cultured in DMEM supplemented with 10% FBS and 1% penicillin/streptomycin. To evaluate a cytotoxicity of the DPP transfersomes and free-Pheo A, NIH/3T3 cells (5×10^3) were incubated with 100 μL of culture medium in 96-well plates. After 24 h, different concentrations of Pheo A and the DPP transfersomes (0.01, 0.1, 1, 10, and 100 μg mL^{-1} of Pheo A) were added to the culture plates and incubated for additional 24 h. Then, MTT solution (0.5 mg mL^{-1}) was treated to the cell culture media and incubated for 4 h. Finally, 1 μL of DMSO was added and the optical density (OD) was measured using Microplate Reader (Bio-Tek, VT, USA). Samples were analyzed in triplicate.

Evaluation of SOG Efficiency: To evaluate the SOG efficiency of the DPP transfersomes in aqueous media, SOSG was added at a concentration of 2.0×10^{-3} M. SOG was induced by irradiation at various light intensities ranging from 0 to 81 J cm^{-2} using a 671 nm fiber-coupled laser system (LaserLab, Korea). After irradiation, SOSG fluorescence was read at an excitation and maximum wavelengths of 540 and 525 nm, respectively. SOG efficiency was evaluated by examining the increase in SOSG fluorescence compared to the background or a control sample.

Skin Penetration Efficiency Test of the DPP Transfersomes: All animal test procedures were approved by the Institutional Animal Care and Use Committee of the Catholic University of Korea (Republic of Korea) in accordance with the "Principles of Laboratory Animal Care," NIH Publication No. 85-23, revised in 1985.

A Franz cell system was built as follows. Six-week-old male Balb/c nude mice (Orient, Korea) were maintained in a well-ventilated environment under controlled temperature (24 ± 1 °C) and humidity (60% ± 5%). Mouse back skins were placed on the upper donor chamber of the diffusion cell, separating the upper compartment from the receptor chamber. Free Pheo A, Pheo A-loaded liposomes, and DPP transfersomes (1.00 μg mL^{-1} of final Pheo A concentration) were treated on the skin with thickness of 1.2 mm and area of 1.77 cm^2 with PBS (0.5 mL, 10×10^{-3} M, pH 7.4). The receptor chamber was maintained at 37 °C and completely filled with PBS (10×10^{-3} M, pH 7.4) to wet the skin and sample. To avoid evaporation, the top plate was tightly sealed. In some of the PBS experiments, the volume of the external medium was completely discarded and refilled with fresh buffer. After 24 h, the skins were embedded in optical cutting temperature (OCT) compound (TISSUE-TEKS 4583; Sakura Finetek USA, Inc.) and frozen. The specimens were cut into 10 μm thick sections at –25 °C and observed using confocal microscopy.

P. acnes Culture: *P. acnes* were cultured on modified reinforced Clostridial medium (mRCM; BD, Franklin Lakes, NJ) at 37 °C in an anaerobic environment. To determine the growth curves, *P. acnes* was diluted and plated on BD agar. The plates were incubated at 37 °C for 1 d in a 10% CO_2 incubator, and the CFU was determined. ODs of 0.1 or 1.0 were measured at 600 nm with an UV–vis spectrometer (UV-2450, Shimadzu, Japan).

In Vitro Measurement of MIC Using Agar Diffusion Assay: To confirm the antibacterial concentration of Pheo A and necessary laser power condition, *P. acnes* suspensions (1×10^9 colony forming units mL^{-1}) were treated with free Pheo A (0–1 μg mL^{-1}) or DPP transfersomes (0–1 μg mL^{-1} of Pheo A concentration). After mixing, the samples were spread on an agar plate, irradiated (0–4 J cm^{-2}), and incubated for 72 h

at 37 °C in an anaerobic environment. The inhibition zone was measured on bacterial culture plates.

In Vitro Antibacterial Effect of the DPP Transfersomes: The stock culture of *P. acnes* was transferred to mRCM broth and incubated anaerobically at 37 °C overnight. The cultures were later used to prepare bacterial suspensions (2×10^6 colony forming units mL^{-1}) in PBS. Subsequently, 100 µL of bacterial suspension was transferred to a 15 mL glass centrifuge bottle, and PBS buffer, free Pheo A, or the DPP transfersomes (1 µg mL^{-1} of final Pheo A concentration) were added. After irradiation at a light intensity of 4 J cm^{-2} (20 mW cm^{-2} and 200 s) using a 671 nm fiber-coupled laser system (LaserLab, Korea), the suspension was spread on an mRCM agar plate. After 72 h, the OD600 of the bacterial suspension was recorded by a microplate reader (Bio-Tek, VT, USA). The experiment was replicated three times under the same conditions.

In Vivo Animal Experiments: To observe the bactericidal effect in vivo, *P. acnes* (2×10^6 CFUs mL^{-1}) was intradermally injected into male 4 week old Balb/c nude mice. After bacterial growth, free Pheo A or DPP transfersomes (Pheo A conc.; 1 µg mL^{-1}) were applied to the infected site. After application, the skin was irradiated with a 671 nm fiber-coupled laser system. The optimal laser dose was selected at 150 J cm^{-2} (110 mW cm^{-2} for 22 min). After irradiation, the therapeutic results of each group were evaluated by measuring the swelling volumes of the skin for 14 d. The swelling volumes and increase in skin thickness were measured using a microcaliper (Mitutoyo, Kanagawa, Japan) at particular times after the bacterial injection and treatment.

Ex Vivo Animal Experiments: Skin tissues were excised from the mice 14 d after sample application, and skin tissues were fixed with a 4% paraformaldehyde solution. Next, 10 µm sectioned skins were stained with hematoxylin and eosin (H&E) for immunohistochemical analysis. All sections were examined by an optical microscope (Axio Imager D2, Carl Zeiss, Thornwood, USA). To determine the number of remaining *P. acnes* in the skin after treatment of the DPP transfersome and laser irradiation, the *P. acnes*-induced skin was cut off and punched with an 8 mm biopsy punch. The *P. acnes*-induced skins were homogenized in 2 mL of sterilized PBS with a tissue grinder. To count the CFUs of *P. acnes*, the spread plate was anaerobically incubated for 72 h at 37 °C, and the OD was measured using a UV-spectrophotometer.

Statistical Analysis: The differences between two means were evaluated using an unpaired two-sided Student's *t*-test, assuming equal or unequal variation in the standard deviations (SDs), as appropriate.

Supporting Information

Supporting Information is available from the Wiley Online Library or from the author.

Acknowledgements

H.P. and J.L. contributed equally to this work. This work was supported by the Technology Innovation Program (no. 10047953, Development of chlorine-based optical medicine for topical agents) funded By the Ministry of Trade, Industry and Energy (MI, Republic of Korea), and a National Research Foundation of Korea (NRF) grant funded by the Korea government (MSIP) (Grant No. 2011-0028726).

Received: July 26, 2016
Revised: September 22, 2016
Published online:

[1] M. Trotta, E. Ugazio, E. Peira, C. Pulitano, *J. Controlled Release* **2013**, *86*, 315.
[2] D. Paithankar, B. H. Hwang, G. Munavalli, A. Kauvar, J. Lloyd, R. Blomgren, L. Faupel, T. Meyer, S. Mitragotri, *J. Controlled Release* **2015**, *206*, 30.
[3] D. Yang, D. Pornpattananangkul, T. Nakatsuji, M. Chan, D. Carson, C.-M. Huang, L. Zhang, *Biomaterials* **2009**, *30*, 6035.
[4] H. Gollnick, W. Cunliffe, D. Berson, B. Dreno, A. Finlay, J. J. Leyden, A. R. Shalita, D. Thiboutot, *J. Am. Acad. Dermatol.* **2003**, *49*, S1.
[5] S. Higaki, *J. Mol. Catal. B: Enzym.* **2003**, *22*, 377.
[6] S. Higaki, S. Morimatsu, M. Morohashi, T. Yamagishi, *Int. J. Antimicrob. Agents* **1998**, *10*, 251.
[7] J. G. Weeks, L. McCarty, T. Black, J. E. Fulton, *J. Invest. Dermatol.* **1977**, *69*, 236.
[8] G. Webster, K. McGinley, J. Leyden, *Br. J. Dermatol.* **1981**, *104*, 453.
[9] C. D. Adair, M. Gunter, T. G. Stovall, G. McElroy, J.-C. Veille, J. M. Ernest, *Obstet. Gynecol.* **1998**, *91*, 165.
[10] K. M. Downey, D. C. de Saintonge, *Br. J. Clin. Pharmacol.* **1986**, *21*, 295.
[11] M. L. Cohen, *Science* **1992**, *257*, 1050.
[12] B. Weisblum, *Antimicrob. Agents Chemother.* **1995**, *39*, 577.
[13] P. S. Stewart, J. W. Costerton, *The Lancet* **2001**, *358*, 135.
[14] A. Russell, *Lancet Infect. Dis.* **2003**, *3*, 794.
[15] M. S. Niederman, *Crit. Care Med.* **2001**, *29*, N114.
[16] M. R. Hamblin, T. Hasan, *Photochem. Photobiol. Sci.* **2004**, *3*, 436.
[17] Z. Malik, J. Hanania, Y. Nitzan, *J. Photochem. Photobiol., B* **1990**, *5*, 281.
[18] R. F. Donnelly, P. A. McCarron, C. M. Cassidy, J. S. Elborn, M. M. Tunney, *J. Controlled Release* **2007**, *117*, 217.
[19] H. Park, K. Na, *Biomaterials* **2013**, *34*, 6992.
[20] C.-S. Lee, W. Park, S.-J. Park, K. Na, *Biomaterials* **2013**, *34*, 9227.
[21] J. Montanari, C. Maidana, M. I. Esteva, C. Salomon, M. J. Morilla, E. L. Romero, *J. Controlled Release* **2010**, *147*, 368.
[22] N. Dragicevic-Curic, D. Scheglmann, V. Albrecht, A. Fahr, *J. Controlled Release* **2008**, *127*, 59.
[23] F. S. G. Praca, W. S. G. Medina, R. Petrilli, M. V. L. B. Bentley, *Curr. Nanosci.* **2012**, *8*, 535.
[24] W. Park, S.-J. Park, K. Na, *Biomaterials* **2011**, *32*, 8261.
[25] J. Kim, O. A. Santos, J.-H. Park, *J. Controlled Release* **2014**, *191*, 98.
[26] H. A. Benson, *Expert Opin. Drug Delivery* **2006**, *3*, 727.
[27] G. Cevc, D. Gebauer, J. Stieber, A. Schätzlein, G. Blume, *Biochim. Biophys. Acta* **1998**, *1368*, 201.
[28] J. Walve, S. Bakliwal, B. R. Rane, S. Pawar, *Int. J. Appl. Biol. Pharm.* **2011**, *2*, 204.
[29] T. N. Demidova, M. R. Hamblin, *Int. J. Immunopathol. Pharmacol.* **2004**, *17*, 245.
[30] X. Ragàs, A. Jiménez-Banzo, D. Sánchez-García, X. Batllori, S. Nonell, *Chem. Commun.* **2009**, 2920.
[31] J. D. Bos, M. M. Meinardi, *Exp. Dermatol.* **2000**, *9*, 165.
[32] G.-D. Zhang, A. Harada, N. Nishiyama, D.-L. Jiang, H. Koyama, T. Aida, K. Kataoka, *J. Controlled Release* **2003**, *93*, 141.
[33] D. E. Dolmans, D. Fukumura, R. K. Jain, *Nat. Rev. Cancer* **2003**, *3*, 380.
[34] T. J. Dougherty, C. J. Gomer, B. W. Henderson, G. Jori, D. Kessel, M. Korbelik, J. Moan, Q. Peng, *J. Natl. Cancer Inst.* **1998**, *90*, 889.
[35] A. M. Fisher, A. L. Murphree, C. J. Gomer, *Lasers Surg. Med.* **1995**, *17*, 2.
[36] G. M. El Zaafarany, G. A. Awad, S. M. Holayel, N. D. Mortada, *Int. J. Pharm.* **2010**, *397*, 164.
[37] G. Cevc, G. Blume, A. Schätzlein, *J. Controlled Release* **1997**, *45*, 211.
[38] G. Cevc, G. Blume, *Biochim. Biophys. Acta* **1992**, *1104*, 226.
[39] D. Verma, S. Verma, G. Blume, A. Fahr, *Eur. J. Pharm. Biopharm.* **2003**, *55*, 271.
[40] S. Perni, P. Prokopovich, J. Pratten, I. P. Parkin, M. Wilson, *Photochem. Photobiol. Sci.* **2011**, *10*, 712.
[41] M. Tanaka, M. Kinoshita, Y. Yoshihara, N. Shinomiya, S. Seki, K. Nemoto, T. Hirayama, T. Dai, L. Huang, M. R. Hamblin, Y. Morimoto, *Photochem. Photobiol.* **2012**, *88*, 227.
[42] Y.-M. Jeon, H.-S. Lee, D. Jeong, H.-K. Oh, K.-H. Ra, M.-Y. Lee, *Life Sci.* **2015**, *124*, 56.
[43] K. S. Kim, W. Park, J. Hu, Y. H. Bae, K. Na, *Biomaterials* **2014**, *35*, 337.
[44] B. Geusens, J. Lambert, S. C. De Smedt, K. Buyens, N. N. Sanders, M. Van Gele, *J. Controlled Release* **2009**, *133*, 214.